

## Intermediate phases observed during decomposition of LiBH<sub>4</sub>

Lene Mosegaard<sup>a</sup>, Bitten Møller<sup>a</sup>, Jens-Erik Jørgensen<sup>a</sup>, Ulrike Bösenberg<sup>b</sup>,  
Martin Dornheim<sup>b</sup>, Jonathan C. Hanson<sup>c</sup>, Yngve Cerenius<sup>d</sup>, Gavin Walker<sup>e</sup>,  
Hans Jørgen Jakobsen<sup>a</sup>, Flemming Besenbacher<sup>a</sup>, Torben R. Jensen<sup>a,\*</sup>

<sup>a</sup> Interdisciplinary Nanoscience Center (iNANO) and Department of Chemistry, University of Aarhus,  
Langelandsgade 140, DK-8000 Århus C, Denmark

<sup>b</sup> Institute for Materials Research, GKSS Research Centre, D-21502 Geesthacht, Germany

<sup>c</sup> Chemistry Department, Brookhaven National Laboratory, Upton, New York 11973, USA

<sup>d</sup> MAX-lab, Lund University, S-22100 Lund, Sweden

<sup>e</sup> School of Mechanical, Materials and Manufacturing Engineering, University of Nottingham, Nottingham NG7 2RD, UK

Received 29 September 2006; received in revised form 10 March 2007; accepted 12 March 2007

Available online 16 March 2007

### Abstract

Lithium tetrahydridoboranate is among the materials with the highest hydrogen content and has great potential as a possible H<sub>2</sub>-storage material, although, the release and uptake of H<sub>2</sub> is not fully understood. In this work, LiBH<sub>4</sub> was studied by in situ synchrotron radiation powder X-ray diffraction (PXD) and solid state CP/MAS NMR both at variable temperatures. This study revealed two new phases observed during dehydrogenation of LiBH<sub>4</sub>. Phase **I** is hexagonal,  $a = 4.93(2)$  and  $c = 13.47(3)$  Å and is observed in the temperature range  $\sim 200$ – $300$  °C, and phase **II** is orthorhombic,  $a = 8.70(1)$ ,  $b = 5.44(1)$  and  $c = 4.441(8)$  Å and is observed in the temperature range  $\sim 300$ – $400$  °C applying a constant heating rate of 5 °C/min. Apparently, **I** transforms into **II**, e.g. at a constant temperature of  $T = 265$  °C after 5 h. Furthermore, a third phase, **III**, is observed in the temperature range  $RT$  to 70 °C, and is caused by a reaction between LiBH<sub>4</sub> and water vapor from the atmosphere. Hydrogen release is associated with the decomposition of **III** at ca. 65 °C.

© 2007 Elsevier B.V. All rights reserved.

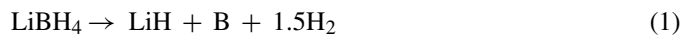
**Keywords:** Energy storage materials; X-ray diffraction

### 1. Introduction

Renewable energy sources are obvious alternatives to the present use of fossil fuels, but unfortunately, their energy outputs are in general not constant in time, and an efficient method of storage is, therefore, of utmost importance for their applicability. Hydrogen is suggested to be a possible energy carrier in the future, but compact, efficient and robust ways to store hydrogen remain an unsolved problem, in particular for mobile applications [1–3].

Solid state storage of hydrogen appears to be the most promising method to achieve both high volumetric and gravimetric storage density. Lithium tetrahydridoboranate, LiBH<sub>4</sub>, is among the materials with the highest theoretical hydrogen contents

measured by mass,  $\rho_m = 18.5$  mass%, and has been intensively studied during the past few years, also as constituent in reactive hydride composites. Still, the exact mechanism for the hydrogen release and uptake is poorly understood. At low temperatures, LiBH<sub>4</sub> exists as an orthorhombic phase, which converts to a high-temperature hexagonal phase at  $\sim 108$  °C, and the material melts at 275 °C [4,5]. This compound can release ca. 14 mass% of hydrogen at elevated temperatures ( $T > 400$  °C) following the equation:



Its use in technological applications is hampered by the relatively high enthalpy change for the reaction,  $\Delta H = 68.9$  kJ/mol H<sub>2</sub> and limited reversibility [6]. The reaction enthalpy can be reduced following the concept of reactive hydride composites, which lowers the dehydrogenation temperature of the material [7–9]. Experimental data suggest the presence of intermediate phases of lithium tetrahydridoboranate, e.g. thermal desorp-

\* Corresponding author. Tel.: +45 8942 3894; fax: +45 8619 6199.  
E-mail address: trj@chem.au.dk (T.R. Jensen).

tion spectra of  $\text{LiBH}_4$  mixed with  $\text{SiO}_2$  show three peaks corresponding to the nominal composition  $\text{LiBH}_{3.6}$ ,  $\text{LiBH}_3$  and  $\text{LiBH}_2$  [10,11]. Recently, the existence of several new lithium boranate phases, e.g.  $\text{LiB}_3\text{H}_8$  and  $\text{Li}_2\text{B}_n\text{H}_n$  ( $n = 5\text{--}12$ ) and others, was proposed based on theoretical calculations [12–15]. Such phases might form during the dehydrogenation of  $\text{LiBH}_4$ .

In this study, we characterize the dehydrogenation of  $\text{LiBH}_4$  and its reaction with moisture using in situ synchrotron radiation powder X-ray diffraction (SR-PXD) and solid state CP/MAS NMR both at variable temperatures and present experimental evidence of the presence of three new phases.

## 2. Experimental

*In situ time resolved synchrotron radiation powder X-ray diffraction (SR-PXD).* Data were collected at the beamline X7B, NSLS, Brookhaven National Laboratory and at I711 at the MAX II synchrotron at MAX-lab, Lund, Sweden with a MAR345 image plate system and a MAR165 CCD detector, respectively [16,17]. The selected wavelengths were in the range of 0.92–1.11 Å, and the X-ray exposure time was 30–60 s. A number of experiments were conducted using a specially constructed sample cell for studies of gas/solid reactions in the temperature range *RT* to 500 °C [18,19]. A sapphire single crystal tube ( $\text{Al}_2\text{O}_3$ , i.d. 0.9 mm) was used as a sample holder. A gas supply system allowing changes in gas and pressure via a vacuum pump was attached to the sample cell. The gas system was flushed with nitrogen and evacuated three times prior to the X-ray experiment. SR-PXD raw data were converted to powder diffraction profiles using the program *FIT2D*, and refinement of cell parameters was performed using the *Fullprof* program [20,21].

*Powder X-ray diffraction (PXD)* data for phase identification were obtained at *RT* in transmission geometry using a Stoe diffractometer,  $\text{Cu K}\alpha_1$  radiation,  $\lambda = 1.54060$  Å, a curved position sensitive detector covering 40° and counting time of 150–500 s/step. Air-sensitive samples were mounted between two thin (3.6 µm) Mylar films. Unfortunately, this set-up was not always completely air tight. Samples for the investigation of the effect of air exposure were mounted on tape.

*Solid state  $^7\text{Li}$ ,  $^{11}\text{B}$  and  $^{13}\text{C}$  CP/MAS NMR spectra* were recorded on a Varian INOVA-400 (9.4 T) spectrometer using a home-built CP/MAS probe for 5 mm o.d.  $\text{Si}_3\text{N}_4$  rotors (110 µL sample volume) and a spinning speed ( $\nu_r$ ) in the range of 3500–5000 Hz. A home-built variable temperature (*VT*) unit operated in the temperature range from *RT* up to 150 °C, using hot nitrogen gas [22,23]. The end cap had a 0.8 mm hole to omit elevated pressures from released gasses. Chemical shifts of  $^7\text{Li}$  and  $^{11}\text{B}$  are given relative to 1 M  $\text{LiCl}(\text{aq})$  and 1 M  $\text{B}(\text{OH})_3(\text{aq})$ .

*Thermogravimetric (TG) and differential scanning calorimetry (DSC)* experiments were performed on a Netzsch STA 449 C Jupiter instrument, with heating rates of 10 °C/min in the temperature range *RT* to 550 °C using aluminum oxide crucibles with lid. Additionally, DSC and TG measurements were performed simultaneously with analysis of the exhaust gas by a Hiden HPR-20 QIC Mass spectrometer mounted on a Netzsch STA 409 C (5 °C/min, the carrier gas was purified argon). The entire apparatus was placed in an argon filled glove box.

*Sample preparation:*  $\text{LiBH}_4$  (95% purity) was purchased from Aldrich Co. and Strem Chemicals. A series of experiments, denoted (A), was performed in order to study the thermal stability of  $\text{LiBH}_4$ . In each case,  $\text{LiBH}_4$  was placed in a crucible of  $\text{Al}_2\text{O}_3$  in a quartz tube, which was evacuated to  $\sim 1 \times 10^{-5}$  mbar and sealed in a hydrogen flame. The quartz tubes were heated for different periods of time, 30 min–30 days, at a constant temperature of 245 or 265 °C. Another series of experiments, (B), was conducted where  $\text{LiBH}_4$  was exposed to air (23 °C, 74% air moisture) for 1–18 min prior to sealing as described above. These quartz tubes were placed at a constant temperature of 265 °C for 1 h. The products were mixed with an internal X-ray standard ( $\text{NaCl}$ , ca. 14 mass%) and analyzed by PXD. All sample preparations were performed in a nitrogen or argon-filled glovebox.  $^{13}\text{C}$  CP/MAS NMR indicates no carbon containing compounds in  $\text{LiBH}_4$  (as received).

## 3. Results

### 3.1. Two new phases observed during dehydrogenation of $\text{LiBH}_4$

Fig. 1 shows a series of SR-PXD patterns of  $\text{LiBH}_4$  heated from *RT* to 340 °C, which show the orthorhombic phase, denoted *o*- $\text{LiBH}_4$ , transforms into the hexagonal polymorph, denoted *h*- $\text{LiBH}_4$  at  $\sim 108$  °C. Six additional reflections are observed in the temperature range 200–300 °C, and they can be indexed on a hexagonal unit cell (Tables 1 and 3). This new phase, denoted **I**, appears to be slightly more stable than *h*- $\text{LiBH}_4$ , which melts at 275 °C. Reflections from **I** disappear at ca. 300 °C when subject to a constant heating rate (e.g. 5 °C/min), possibly due to dissolution in molten  $\text{LiBH}_4$ . Furthermore, a powder pattern consisting of seven new reflections indexed on an orthorhombic unit cell was observed at 300–400 °C, which is possibly due to the formation of another new phase, denoted **II** (Tables 2 and 3).

In addition to the in situ SR-PXD measurements, a series of experiments (A) was performed by heating  $\text{LiBH}_4$  in sealed quartz tubes at 265 °C for different time intervals in order to study the formation of **I** and **II** by ex situ PXD as shown in Fig. 2. After 1 h of annealing only a small amount of **I** is present, and after 5 h, **I** is transformed into phase **II**, and both phases were found to be stable at *RT*. Similar results were obtained at 245 °C at slightly longer heating times. Only a moderate amount of **I** and

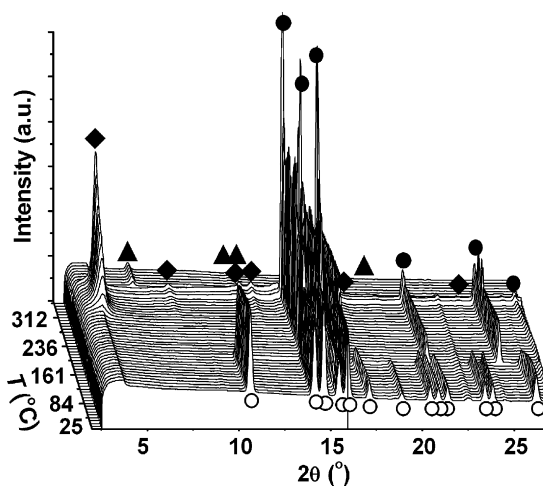


Fig. 1. In situ SR-PXD of  $\text{LiBH}_4$  heated from *RT* to ca. 340 °C (heating rate  $\sim 5$  °C/min,  $\lambda = 0.92172$  Å). Symbols: (◆) phase **I**, (▲) phase **II**, (○) *o*- $\text{LiBH}_4$  and (●) *h*- $\text{LiBH}_4$ .

Table 1

Indexed PXD pattern for phase **I** using the unit cell parameters given in Table 3 (data measured at 263 °C,  $\lambda = 0.92172$  Å)

$2\theta_{\text{obs}}$ (°)	HKL	$2\theta_{\text{calc}}$ (°)	$2\theta_{\text{obs}} - 2\theta_{\text{calc}}$ (°)	<i>I</i> (%)	$d_{\text{obs}}$ (Å)	$d_{\text{calc}}$ (Å)
3.911	0 0 1	3.920	−0.0088	100	13.5044	13.4742
7.872	0 0 2	7.845	0.027	30.1	6.7135	6.7371
11.760	0 0 3	11.779	−0.0191	29.6	4.4987	4.4914
12.376	1 0 0	12.393	−0.0163	29.3	4.2753	4.2697
17.152	1 0 3	17.129	0.0224	25.2	3.0905	3.0946
23.679	0 0 6	23.685	−0.0057	23.1	2.2462	2.2457

Table 2

Indexed PXD pattern for phase **II** using the unit cell parameters given in Table 3 (data measured at 327 °C,  $\lambda = 0.92172 \text{ \AA}$ )

$2\theta_{\text{obs}}$ (°)	HKL	$2\theta_{\text{calc}}$ (°)	$2\theta_{\text{obs}} - 2\theta_{\text{calc}}$ (°)	$I$ (%)	$d_{\text{obs}}$ (Å)	$d_{\text{calc}}$ (Å)
6.066	100	6.069	-0.0028	100	8.710	8.7059
11.456	110	11.463	-0.0072	77.4	4.6176	4.6147
11.926	001	11.914	0.0117	75.4	4.4362	4.4405
15.595	210	15.584	0.0110	70.0	3.3969	3.3993
16.561	111	16.562	-0.0014	65.8	3.2000	3.1997
17.037	201	17.052	-0.0151	64.3	3.1112	3.1085
18.279	300	18.276	0.0039	62.2	2.9014	2.9020

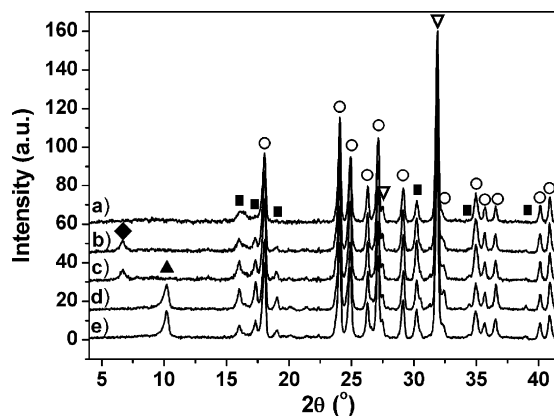


Fig. 2. Ex situ PXD data for  $\text{LiBH}_4$  heated at 265 °C for different periods of time in evacuated sealed quartz tubes. Phase **III** is possibly formed during the PXD measurement (experiments series A, PXD data measured at RT,  $\lambda = 1.5406 \text{ \AA}$ ): (a) not heated  $\text{LiBH}_4$  (as received), (b) heated for 30 min, (c) 1 h, (d) 5 h and (e) 10 h. Symbols: (◆) phase **I**, (▲) phase **II**, (■) phase **III**, (○) *o*- $\text{LiBH}_4$  and (▽) NaCl.

**II** was formed in these experiments, and only a small change in the diffracted intensity from *o*- $\text{LiBH}_4$  was observed. Table 3 summarizes unit cell parameters for the polymorphs of  $\text{LiBH}_4$  and the new phases observed in this study.

### 3.2. Lithium tetrahydridoboranate in contact with the ambient atmosphere

Occasionally, a few reflections were observed in the temperature range RT to 70 °C, as seen from Fig. 3. This phase is denoted **III**. Further experimental studies seen in Fig. 4 clearly demonstrated a correlation between the time of exposure of  $\text{LiBH}_4$  to air and the formation of phase **III**. After prolonged exposure to

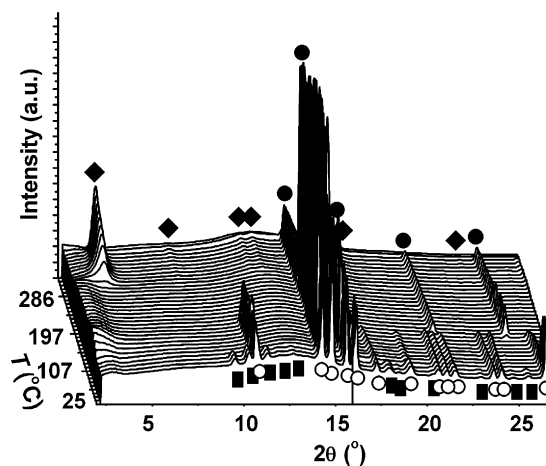


Fig. 3. In situ SR-PXD of  $\text{LiBH}_4$  heated from RT to ca. 290 °C (heating rate  $\sim 3 \text{ °C/min}$ ,  $\lambda = 0.92191 \text{ \AA}$ ). Symbols: (◆) phase **I**, (■) phase **III**, (○) *o*- $\text{LiBH}_4$  and (●) *h*- $\text{LiBH}_4$ .

air, **III** converts to an amorphous material, which later forms an unidentified or new crystalline phase.

Thermal analysis (TG/DSC) of a sample of  $\text{LiBH}_4$  (as received) shows a minor mass loss starting at 56 °C, and no mass loss was detected after the second cycle of TG/DSC without removing the sample from the instrument (Fig. 5). Then this sample was exposed to air 5 min and revealed a mass loss of 1.3 mass% ( $55 \text{ °C} < T < 110 \text{ °C}$ ). The corresponding DSC curve

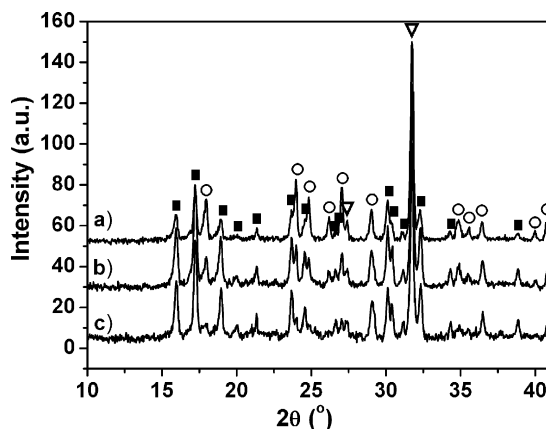


Fig. 4.  $\text{LiBH}_4$  exposed to air for (a) 1 min, (b) 3 min and (c) 5 min and investigated by ex situ PXD. Phase **III** is possibly formed during the PXD measurement (data measured at RT,  $\lambda = 1.5406 \text{ \AA}$ ). Symbols: (■) phase **III**, (○) *o*- $\text{LiBH}_4$  and (▽) NaCl.

Table 3

Unit cell parameters for known polymorphs of  $\text{LiBH}_4$  and phases observed during dehydrogenation of  $\text{LiBH}_4$

Phase	Symmetry	$a$ (Å)	$b$ (Å)	$c$ (Å)	$V$ (Å <sup>3</sup> )	$T$ (°C)	References
<i>o</i> - $\text{LiBH}_4$	Orthorhombic	7.17858(4)	4.43686(2)	6.80321(4)	216.685(3)	20	[5]
<i>o</i> - $\text{LiBH}_4$	Orthorhombic	7.1942(8)	4.4465(5)	6.8193(7)	218.1	25	(a)
<i>h</i> - $\text{LiBH}_4$	Hexagonal	4.27631(5)	4.27631(5)	6.94844(8)	110.041(4)	135	[5]
<i>h</i> - $\text{LiBH}_4$	Hexagonal	4.2991(2)	4.2991(2)	6.9922(6)	111.9	200	(a)
<b>I</b>	Hexagonal	4.93(2)	4.93(2)	13.47(3)	283(2)	263	(a)
<b>II</b>	Orthorhombic	8.70(1)	5.44(1)	4.441(8)	210(1)	327	(a)

(a) This work.

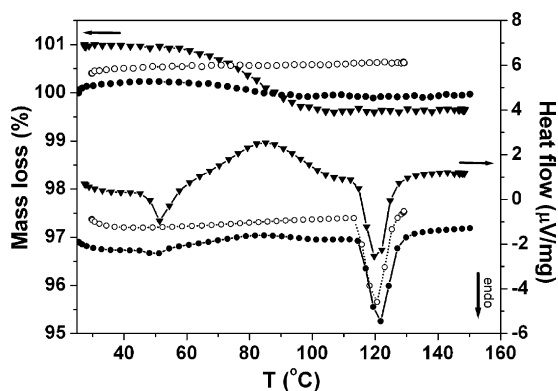


Fig. 5. Three thermal analysis experiments, TG (upper three curves) and DSC, on the same sample of  $\text{LiBH}_4$  (heating rate  $\sim 10^\circ\text{C}/\text{min}$ , the curves are displaced for clarity). Three heating cycles are shown: (a) as received ( $\bullet$ ), (b) second cycle ( $\circ$ ), and (c) the third heating after 5 min exposure to air ( $\blacktriangledown$ ).

shows an endothermic reaction at  $\sim 48^\circ\text{C}$  followed by a broad exothermic signal. Furthermore, these measurements confirm the phase transformation between *o*- and *h*- $\text{LiBH}_4$  at  $\sim 115^\circ\text{C}$ . A similar DSC experiment with mass spectroscopic analysis of the released gas on a sample of  $\text{LiBH}_4$  exposed to air 10 min revealed hydrogen release at  $\sim 61^\circ\text{C}$  simultaneously with the exothermic DSC signal (Fig. 6).

### 3.3. Solid state CP/MAS NMR investigation of phases I and II

Samples of  $\text{LiBH}_4$  and  $\text{LiBH}_4$  containing I or II were investigated by  $^7\text{Li}$  and  $^{11}\text{B}$  CP/MAS NMR at room temperature, and the chemical shifts for these samples were identical (i.e.  $\delta(^7\text{Li}) = -0.88$  ppm and  $\delta(^{11}\text{B}) = -41.01$  ppm) [24]. The line width (FWHM) of  $^7\text{Li}$  and  $^{11}\text{B}$  MAS NMR signals for pure *o*- $\text{LiBH}_4$  increases from 660 to 798 Hz and 369 to 595 Hz, respectively, in the temperature interval *RT* to  $116^\circ\text{C}$ , but decreases abruptly to 36 and 70 Hz, respectively, at the phase transition to *h*- $\text{LiBH}_4$ .  $^{11}\text{B}$  CP/MAS NMR for samples containing II exhibits a larger line width of 622 Hz measured at  $130^\circ\text{C}$ , whereas the other line widths for  $^7\text{Li}$  and  $^{11}\text{B}$  CP/MAS

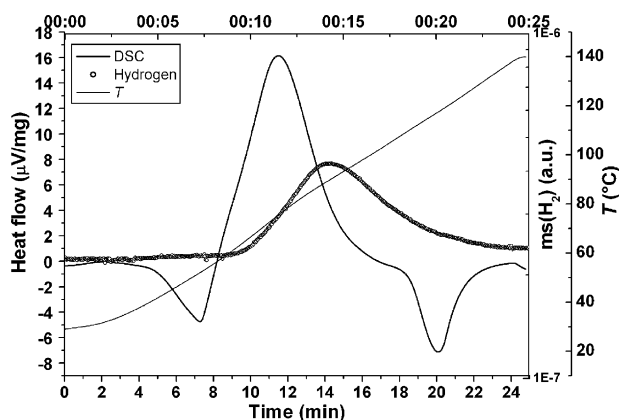


Fig. 6. Thermal analysis (DSC/MS) of  $\text{LiBH}_4$  exposed to the atmosphere for 10 min (heating rate  $\sim 5^\circ\text{C}/\text{min}$ ).

NMR signals for samples containing I and II were similar to *h*- $\text{LiBH}_4$ . A  $^{11}\text{B}$  MAS NMR spectrum of pure  $\text{LiBH}_4$  exposed shortly to air revealed the presence of an impurity (0.3 mass%),  $\delta(^{11}\text{B}) = -3.5$  ppm.

## 4. Discussion

In this work, experimental methods are utilised to explore the nature of two new phases observed during heating of  $\text{LiBH}_4$ . The partial phase transition of  $\text{LiBH}_4$  to phase I is slow, and the limited PXD data does not yet allow a complete structural analysis. I was observed to transform into II, either when kept at a fixed temperature, e.g.  $265^\circ\text{C}$  for 5 h, or when heated constantly, e.g.  $5^\circ\text{C}/\text{min}$  at ca.  $300^\circ\text{C}$ . In this study, no indications of impurities in the used  $\text{LiBH}_4$  were observed, therefore, we suggest that I and II are formed by partial dehydrogenation of  $\text{LiBH}_4$ , which could have slightly lower hydrogen content than stoichiometric  $\text{LiBH}_4$ . The observed X-ray data for phases I and II did not correspond to any of the recently proposed new lithium tetrahydridoboranate materials found by the theoretical calculations [12–15].

Phases I and II are observed independently of the observation of phase III as shown in a series of experiments (B) illustrated in Fig. 7. We demonstrate that there is no correlation between the time of exposure of the sample to the ambient atmosphere and the amount of phases I and II formed.

$^7\text{Li}$  and  $^{11}\text{B}$  CP/MAS NMR spectra of  $\text{LiBH}_4$ ,  $\text{LiBH}_4 + \text{I}$  and  $\text{LiBH}_4 + \text{II}$  show that the chemical shift values are very similar for all three samples in contrast to FWHM for the signals that show some differences. This observation indicates that the Li and B coordination in phases I and II are somewhat similar to those found in  $\text{LiBH}_4$ . These observations will be further investigated [25].

A dihydrogen bonded complex of  $\text{LiBH}_4 \cdot \text{TEA}$  (TEA = triethanolamine) is described in the literature. It decomposes at app.  $120^\circ\text{C}$  during release of hydrogen to the  $\text{BH}(\text{OR})_3^-$  ion, the two compounds have  $^{11}\text{B}$  MAS NMR

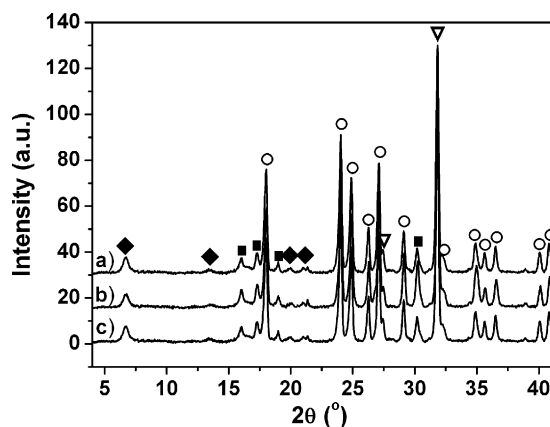


Fig. 7. Ex situ PXD measurement of  $\text{LiBH}_4$  exposed to the atmosphere for different periods of time and afterwards heated to  $265^\circ\text{C}$  for 1 h (experiments series B, data measured at *RT*,  $\lambda = 1.5406 \text{ \AA}$ ): (a)  $\text{LiBH}_4$  exposed to the atmosphere for 1 min, (b) for 5 min and (c) for 18 min. Symbols: ( $\blacklozenge$ ) phase I, ( $\blacksquare$ ) phase III, ( $\circ$ ) *o*- $\text{LiBH}_4$  and ( $\blacktriangledown$ ) NaCl.



chemical shifts of  $\delta(^{11}\text{B}) = -48.0$  and  $-3.9$  ppm, respectively [26]. Furthermore, boron NMR revealed a minor signal at  $\delta(^{11}\text{B}) \approx -3.5$  ppm (in this case 0.3%), which might be **III**. Phase **III** can possibly be a complex between water and  $\text{LiBH}_4$ , e.g. from a surface reaction of water vapor and  $\text{LiBH}_4$  in accordance with the observed hydrogen release during decomposition of **III** at ca.  $65^\circ\text{C}$ . Phase **III** was observed as an impurity in Figs. 2–4, possibly due to exposure of the sample to the atmosphere after the thermal treatment and prior to the PXD. It has not yet been possible to identify or index phase **III**, and it may actually consist of several co-existing phases.

## 5. Conclusion

The hydrogen release and uptake of  $\text{LiBH}_4$  is not yet fully understood. In this work, we have, by means of experimental methods (PXD and MAS NMR), explored the nature of two new phases denoted **I** and **II** suggested to be formed by partial dehydrogenation of  $\text{LiBH}_4$ . Furthermore, **I** was observed to transform into **II**, either when kept at a fixed temperature, e.g.  $265^\circ\text{C}$  for 5 h, or when heated constantly, e.g.  $5^\circ\text{C}/\text{min}$  at ca.  $300^\circ\text{C}$ . Phases **I** and **II** have possibly slightly lower hydrogen content than compared to  $\text{LiBH}_4$ .

An additional phase **III** is observed in the temperature range  $RT$  to ca.  $70^\circ\text{C}$  is suggested to be a complex between water and  $\text{LiBH}_4$ . PXD patterns recorded at  $RT$  showed that the amount of phase **III** scales with the time  $\text{LiBH}_4$  was exposed to the atmosphere. Thermal analysis showed that the decomposition of **III** is associated with release of hydrogen suggesting the presence of dihydrogen bonds in **III**. Finally, we showed that **I** and **II** form independently of the presence of **III**.

## Acknowledgements

The work at BNL was supported by US DOE under contract DE-AC02-98CH10886. TRJ gratefully acknowledges the Carlsberg Foundation for financial support. DANSYNC and the Danish Natural Science Research Council are gratefully acknowledged for financial support.

## References

- [1] L. Schlapbach, A. Züttel, *Nature* 414 (2001) 353.
- [2] Andreas Züttel, *Naturwissenschaften* 91 (2004) 157.
- [3] M. Dornheim, N. Eigen, G. Barkhordarian, T. Klassen, R. Bormann, *Adv. Eng. Mater.* 8 (2006) 377.
- [4] J-Ph. Soulié, G. Renaudin, R. Cerný, K. Yvon, *J. Alloys Compd.* 346 (2002) 200.
- [5] A. Züttel, S. Rentsch, P. Fischer, P. Wenger, P. Sudan, Ph. Mauron, Ch. Emmenegger, *J. Alloys Compd.* 356–357 (2003) 515.
- [6] M.B. Smith, G.E. Brass Jr., *J. Chem. Eng. Data* 8 (1963) 342.
- [7] U. Bösenberg, S. Doppiu, L. Mosegaard, G. Barkhordarian, N. Eigen, A. Borgschulte, T.R. Jensen, Y. Cerenius, O. Gutfleisch, T. Klassen, M. Dornheim, R. Bormann, *Acta Materialia*, 2007, in press.
- [8] G. Barkhordarian, T. Klassen, M. Dornheim, R. Bormann, *J. Alloys Compd.* 440 (2007) L28.
- [9] J.J. Vajo, S.L. Skeith, F. Mertens, *J. Phys. Chem. B, Lett.* 109 (2005) 3719–3722.
- [10] A. Züttel, P. Wenger, S. Rentsch, P. Sudan, Ph. Mauron, Ch. Emmenegger, *J. Power Sources* 118 (2003) 1.
- [11] N. Ohba, K. Miwa, M. Aoki, T. Noritake, S. Towata, Y. Nakamori, S. Orimo, A. Züttel, *Cond. Mat.* (2006), 0606228.
- [12] Z. Lodziana, T. Vegge, *Phys. Rev. Lett.* 93 (2004) 145501.
- [13] J.K. Kang, S.Y. Kim, Y.S. Han, R.P. Muller, W.A. Goddard III, *Appl. Phys. Lett.* 87 (2005) 111904.
- [14] N. Ohba, K. Miwa, M. Aoki, T. Noritake, S. Towata, *Phys. Rev. B* 74 (2006) 075110.
- [15] T.J. Frankcombe, G.-J. Kroes, A. Züttel, *Chem. Phys. Lett.* 405 (2005) 73.
- [16] J.B. Hastings, P. Suortii, P. Thomsolin, A. Kvik, T. Koetzle, *Nucl. Instrum. Methods* 208 (1993) 55.
- [17] Y. Cerenius, K. Ståhl, L.A. Svensson, T. Ursby, Å. Oskarsson, J. Albertsson, A. Lijas, *J. Synchrotron Radiat.* 7 (2000) 203.
- [18] B.S. Clausen, G. Steffensen, B. Fabius, J. Villadsen, R. Feidenhans'l, H. Topsøe, *J. Catal.* 132 (1991) 524.
- [19] J.A. Rodríguez, J.C. Hanson, A.I. Frenkel, J.Y. Kim, M. Perez, *J. Am. Chem. Soc.* 124 (2002) 346.
- [20] J. Rodríguez-Carvajal, *Physica B* 192 (1993) 55.
- [21] A.P. Hammersley, Internal Report, ESRF-97-HA02T, 1997.
- [22] (a) H.J. Jakobsen, P. Daugaard, V. Langer, *J. Magn. Reson.* 76 (1988) 162; (b) H.J. Jakobsen, P. Daugaard, V. Langer, U.S. Patent 4, 739, 270 (1988).
- [23] J. Skibsted, N.C. Nielsen, H. Bildsøe, H.J. Jakobsen, *J. Magn. Reson.* 95 (1991) 88.
- [24] S.R. Johnson, P.A. Anderson, P.P. Edwards, I. Gameson, J.W. Prendergast, M. Al-Mamouri, D. Book, I.R. Harris, J.D. Speight, A. Walton, *Chem. Commun.* (2005) 2823.
- [25] T.R. Jensen, L. Mosegaard, B. Møller, J.E. Jørgensen, Y. Cerenius, J.C. Hanson, F. Besenbacher, H.J. Jakobsen, (2007) to be submitted.
- [26] R. Custelcean, J.E. Jackson, *J. Am. Chem. Soc.* 122 (2000) 5251.